Final Report DE-FG02-08ER85042
Modeling Electron Cloud Diagnostics for High-Intensity Proton Accelerators

Seth A. Veitzer, P.I.
Tech-X Corporation
5621 Arapahoe Ave. Suite A
Boulder, CO 80303

Performance Period: June 30, 2008 - July 31, 2009
Grant supported by DOE Office of High Energy Physics

September 25, 2009

Executive Summary

Future experiments to study high energy physics require the construction of new, high-intensity particle accelerators that are pushing the frontiers of accelerator design. Electron cloud effects are considered to be one of the most important factors that will limit machine performance for high-intensity accelerators, and electron cloud mitigation methods can have a large influence on the cost and design of such accelerators. Recently, researchers have developed a new diagnostic technique that uses microwaves to measure electron cloud densities [1, 2, 3], and there are a number of experimental programs both in the United States (FermiLab, SLAC, LBL, Cornell) and abroad (CERN) that are using injected microwaves to measure both electron cloud densities and the effects of cloud mitigation techniques, such as coatings to reduce production of secondary electrons.

However, understanding in detail the results of this diagnostic requires accounting for the specifics of the each different machine, such as beam pipe cross section and magnetic field location and strength. Simulation is a possible method for reducing the cost and time required to field a microwave electron cloud diagnostic. In addition, accurate simulation of the behavior of higher order RF modes and plasma resonances may provide new designs that will help researchers more accurately measure electron clouds and the effectiveness of different mitigation techniques. Finally, simulation is a powerful tool for understand the fundamentals of electron cloud formation. The goal of this work is to provide the simulation tools necessary to help accelerator physics researchers field effective microwave electron cloud diagnostics, including understanding cloud formation, so that they may reduce the negative effects of electron clouds in current and future high-intensity accelerators. The success of the Phase I project showed that the overall Phase II goals were feasible and that the Phase II project had a high chance of success.

Tech-X Corporation has developed a plasma simulation package, called VORPAL [4] that we used extensively in the Phase I project to numerically model the propagation of microwaves through beam pipes containing electron plasmas. In the Phase I project we extended both the physics and geometry to more accurately model electron cloud diagnostics relevant to high-intensity proton accelerators. Further, we showed VORPAL simulations can model the details of electron cloud formation for parameters relevant to the Main Injector at Fermilab, including the effectiveness of different magnetic field configurations as a mitigation technique. The flexibility and parallel capabilities of VORPAL formed a firm foundation for producing accurate and detailed results for this complex modeling challenge.

The Phase I Technical Results

The overall objective of this work was to improve modeling of microwave diagnostics for measuring electron clouds and to provide experimentalists with the tools to design better RF diagnostics and measure the effectiveness of electron cloud mitigation techniques. There were three technical objectives in the Phase I project, that we successfully achieved.

Objective 1: Determine if non-uniform electron cloud densities and higher-order TE-TM modes could improve microwave transmission diagnostics

Objective 2: Determine if externally applied magnetic fields affect microwave transmission diagnostics

Objective 3: Demonstrate the ability to measure electron cloud densities in realistic geometries relevant to current and future accelerators

Developing a full simulation capability was beyond the scope of the Phase I project, so we focussed on particular subsets of the problem that we considered to be the most important for demonstrating that the overall project will succeed: non-uniform cloud densities, higher-order EM modes, differing magnetic fields, and realistic beam pipe geometries.

We achieved the Phase I objectives by successfully carrying out the tasks proposed for the Phase I. The research results for the Phase I project demonstrated the technical feasibility of successfully carrying out the overall project objectives. These results are discussed in detail below.

Task 1: Demonstrate transmission of EM waves through an electron cloud in a beam pipe with curved boundaries

It was sensible to achieve this task prior to the others, so that the other tasks would include higher-fidelity physics associated with realistic beam pipe geometries. The parameterizations for other studies such as determining the effects of higher order modes depends intimately on the geometry. For instance, the cut off frequencies of higher order modes depend on whether the beam pipe has circular or elliptical cross section. In order to accurately study the feasibility of using higher order modes to measure cloud densities we felt that it was important to first model beam pipes with curved boundaries.

To achieve this task we first implemented numerically stable algorithms for particle absorption and emission from cut-cell boundaries, and verified that these algorithms were consistent with EM field boundary conditions in VORPAL. Once these methods were verified, we were able to design a general input file for simulating propagation of microwaves in an electron plasma with varying densities, arbitrary external magnetic fields, and for a variety of realistic geometries, including circular and elliptical cross section beam pipes.

The geometry of this and subsequent simulations can be seen in figure (1). The same general geometry was used for most of the simulations, but we did perform a simulations using both circular and elliptical cross section beam pipes. In the center of the beam pipe there is an electron cloud, whose properties can be varied from simulation to simulation run. To the left of the electron cloud there is a prescribed current source which launches an RF signal through the electron cloud. The frequency, polarization, and strength of the RF wave can also be varied. To simulate a traveling wave through the electron cloud, we place Perfectly Matched Layers (PMLs) on the left and right ends of the beam pipe. These unphysical layers absorb electromagnetic energy so that none of the RF signal is reflected back through the electron cloud. In addition, electrons are absorbed at the PML surface, and at the beam pipe surface. We also simulate secondary electron emission from the beam pipe surfaces in long-duration simulations where the electrons may hit the walls. Optionally, we can inject a beam current down the beam pipe to simulate the effects on the electron cloud, primarily the evolution of cloud density. By measuring the RF signal after it has passed through the electron cloud, and comparing that signal to one for which there is no electron cloud, we compute the phase shift induced by the plasma.

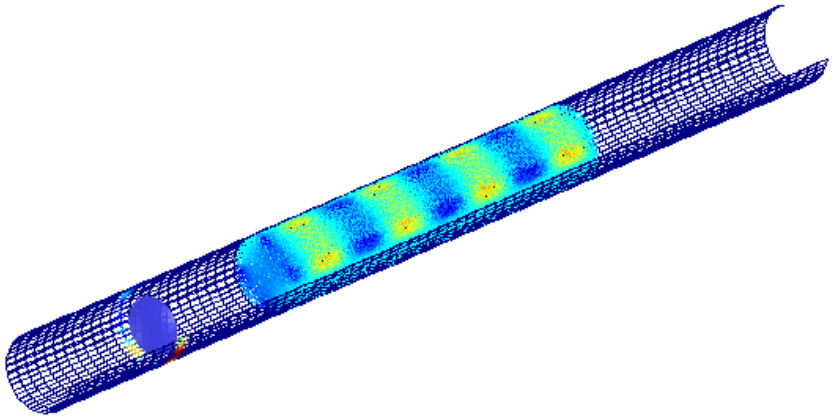

Figure 1: Representation of typical simulation geometry. The blue disk is the location of the current source that creates the RF signal. Electrons in the beam pipe are colored here by their y-momentum, showing that as the RF signal propagates through the electron cloud, the initially uniform density and cold cloud gains some momentum from the RF wave.

In this task we verified that fields and particles in the simulation interact with the simulation boundaries in a numerically stable way. We used cut-cell boundaries to model the beam pipe walls. Second-order accurate algorithms ensure that EM fields are numerically stable at the boundary. In this task, we also verified that new algorithms for absorbing and emitting particles from cut-cell boundaries we able to add and remove charge from the simulation without leaving excess, non-physical charge on the computational grid. These tests, coupled with long-term simulations with beam bunches included showed that the particle-surface algorithms work with cut-cell geometries, and that it was feasible to use cut-cells to model curved geometry in electron cloud diagnostic simulations, such as circular and elliptical cross-section beam pipes.

The cut-cell algorithms in VORPAL allow users to modify the simulation in order to make it more stable when there are cut cells. The time step in explicit PIC simulations is limited by the size of the cell. The Courant-Friedrichs-Lewy (CFL) condition sets the discrete time step such that light crosses only some fraction of a cell during one time step. This ensures numerical stability in the underlying Yee Finite Difference Time Domain (FDTD) algorithms. With the typical electron plasma densities that we are interested in here, namely $\sim 10^{11} - 10^{13} \#/m^3$, we typically choose a computational cell size to be on the order of a tenth of a millimeter in the

transverse direction. The beam pipe radius is typically on the order of a few centimeters, and this choice sets the Debye length so that the plasma does not artificially heat up very much due to numerical instabilities (grid heating). We chose the number of cells in the beam propagation direction such that we can resolve the spatial extent of the RF wave, typically on the order of 1 mm or less. Given the CFL condition, the time step is computed from the cell sizes, and is typically on the order of 1 - 10 ps.

With cut cells, the actual beam pipe wall may slice off a very small piece of a computational cell, reducing the time step for the entire simulation. One way to fix this is to specify a volumetric fraction, below which cut cells are rejected and stair stepped instead. This allows the user to strike a balance between accuracy of the fields and simulation performance. We tested the stability of both fields and particles in the cut-cell simulation geometry in Phase I. We found that the particle trajectories are not particularly sensitive to the granularity of the fields at the cut-cell boundaries, especially for cold electrons, which start off with no kinetic energy at the beginning of the simulation. This is primarily due to the fact that the amplitude of the RF signal overwhelms any small errors induced in the EM fields due to stair-stepped approximations at the boundary. This is also a benefit because we are considering very simple geometries, namely circular and elliptical cross section cylinders. In future simulations with more complicated geometries, it will be important to reduce the granularity of the beam pipe walls in order to accurately compute the fields. In terms of computing phase shifts, our method was not at all sensitive to static errors in the fields because they are subtracted out when comparing to the case with no electrons in order to compute phase shifts.

Task 2: Model propagation of higher-order EM modes through non-uniform electron clouds

We successfully completed this task during the Phase I project. We modified the RF signal by changing both the frequency of the driving current source as well as the direction, so we were able to specify the frequency and polarization of the RF signal in our simulations. In most of these simulations, the beam pipe has circular cross section with radius $r = 4.45$ cm. We also simulated elliptical cross section beam pips with major radius 5.8801 cm and minor radius 2.3876 cm relevant to the Main Injector. For the circular cross section beam pipes, The TE11 mode has a cutoff frequency of $f_c(TE_{11}) = 1.8412c/r = 1.974$ GHz. We drove current in the y-direction (perpendicular to the beam propagation direction) with a frequency of 1.994 GHz, about 10% above the cutoff frequency, exciting only the TE11 mode. Similarly the TM01 mode has a cutoff frequency of 2.578 GHz, and we drive the current source at 2.836 GHz in the x-direction (propagation direction) to excite only that mode. Samples of the wave amplitudes for these modes are shown in figures (2) and (3). Figure (2) shows the components of electric and magnetic fields for TE11 RF signals. Similarly figure (3) shows the field components for the TM01 mode.

We first measured the phase shifts for TE11 and TM01 modes in circular cross section beam pipes for uniform density electron clouds. The results are shown in figure (4), which shows the computed phase shifts induced by electron clouds as a function of cloud density for both the TE11 and TM01 modes. As is expected, the phase shift per unit length increases linearly with cloud density. Overall, the magnitude of the phase shift is smaller for TM01 modes. We believe that the magnitude of the phase shift depends on the strength of the transverse electric field,

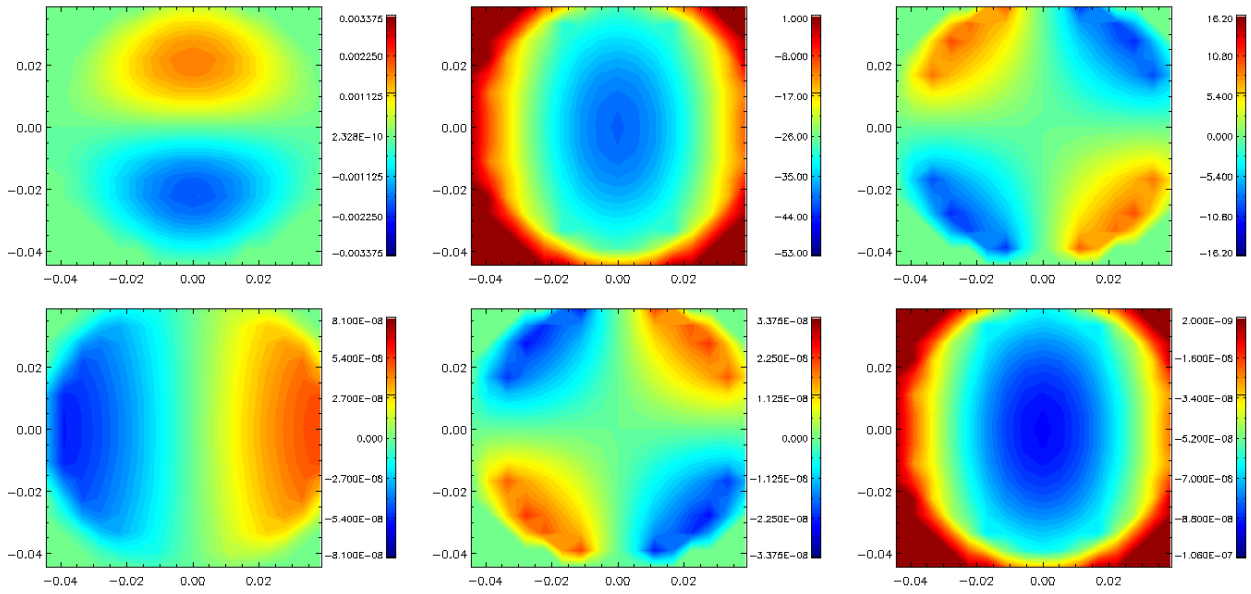

Figure 2: TE11 electric and magnetic field components. Top row (left to right): E_x, E_y, E_z. Bottom row (left to right): B_x, B_y, B_z. Notice that the x-component (longitudinal) of the electric field is very small compared to the transverse components. The existence of any longitudinal electric field in at TE mode is due to numerical errors stemming from driving the wave with a finite-sized dipole current source, rather than launching a plane wave from the simulation boundaries. This amount of error is acceptable and does not negatively effect the ability to accurately measure induced phase shifts.

and since the average strength of transverse electric fields is greater in TE modes, we indeed observed a larger phase shift for TE modes.

We next considered the phase shifts for non-uniform density electron clouds. For this part of the task, we generated electron clouds that were non-uniform, with a continuously varying density as a function of radius r given by

$$\rho(r) = 1 - \exp[-(r/R_0)^2/\sigma^2] \tag{1}$$

where R_0 is the beam pipe radius and σ is a form factor. The cloud is uniform density when $\sigma = 0$, and becomes more skewed to larger radius when σ increases. The left plot in figure (5) shows the density profile as a function of radius for a number of different non-uniformity factors.

We measured the induced phase shifts for TE11 and TM01 modes as a function of non-uniformity in the electron cloud density, which is shown in figure (5). In both cases the greatest phase shift is seen for uniform density clouds. There are two reasons for this. First, the overall cloud density is greater in these cases. Secondly, TE11 and TM01 modes both have large transverse electric fields in near the center of the beam pipe. Referring to figure (5), it is evident that clouds with a small σ have a higher density near the center of the beam pipe. It is not easy to discern between the two effects in this case. Thus we looked at a different scenario to measure the effect of non-uniform cloud density on the induced phase shifts.

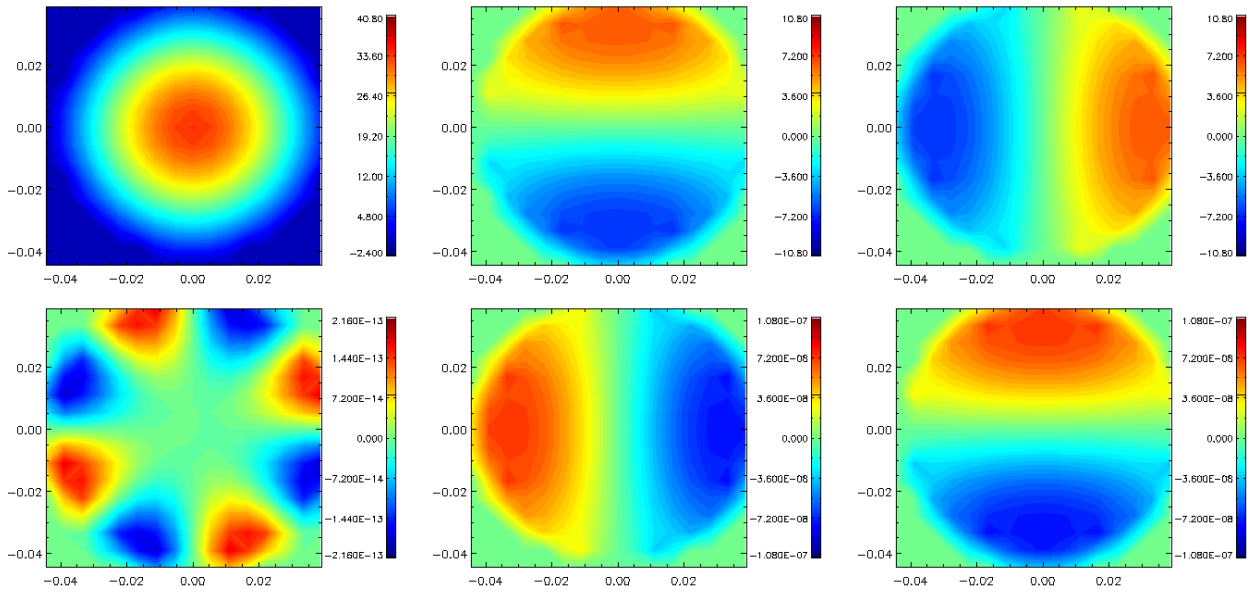

Figure 3: TM01 electric and magnetic field components. Top row (left to right): E_x, E_y, E_z. Bottom row (left to right): B_x, B_y, B_z. In this case the current source is driven in the propagation direction, exciting a TM mode. Although the driving frequency is above that of the TE11 mode, that mode is not excited here. The electric field has large components in all three directions. B_x is about six orders of magnitude smaller than the transverse components of the magnetic field, indicating a nearly completely TM mode.

To simulate the effect, we first distributed annular rings of uniform density electrons in the beam pipe at different radii, and measured the phase shifts for these clouds. The rings all had constant area, so that the overall density of electrons sampled by the RF waves was the same from simulation to simulation. Figure (6) shows an example of the geometry of these simulations.

We then computed the phase shift for various higher-order modes propagating through these clouds of electrons as a function of the radius of the centroid of the cloud. The results are shown in figure (7). We find that there are consistently peaks in the phase shift corresponding to the antinodes of the transverse electric field of the wave, with minimums close to the zero points of the EM mode. For instance, referring to figure (7), there are two peaks in the phase shift for TM02 mode, and three peaks for TE13 and TM03 modes. These observations support the conjecture that it is the interaction of the transverse electric field with the electron plasma that is responsible for inducing the phase shift.

Although it may be intuitive that there should be a larger phase shift when the electrons are in a spatial location where there is a stronger electric field, it has yet to be shown theoretically how higher order modes are sensitive to spatially non-uniform plasma densities. A likely method for showing this is to first compute the perturbation of the vacuum solutions for propagating waves in a circular cross section beam pipe. These solutions would then form a basis for computing the spatial mixing of modes due to the plasma interaction. It may be possible in the future to inject multiple higher-order modes into accelerator beam pipes at the same time, and reconstruct the spatial patterns of electron cloud density using the above observations.

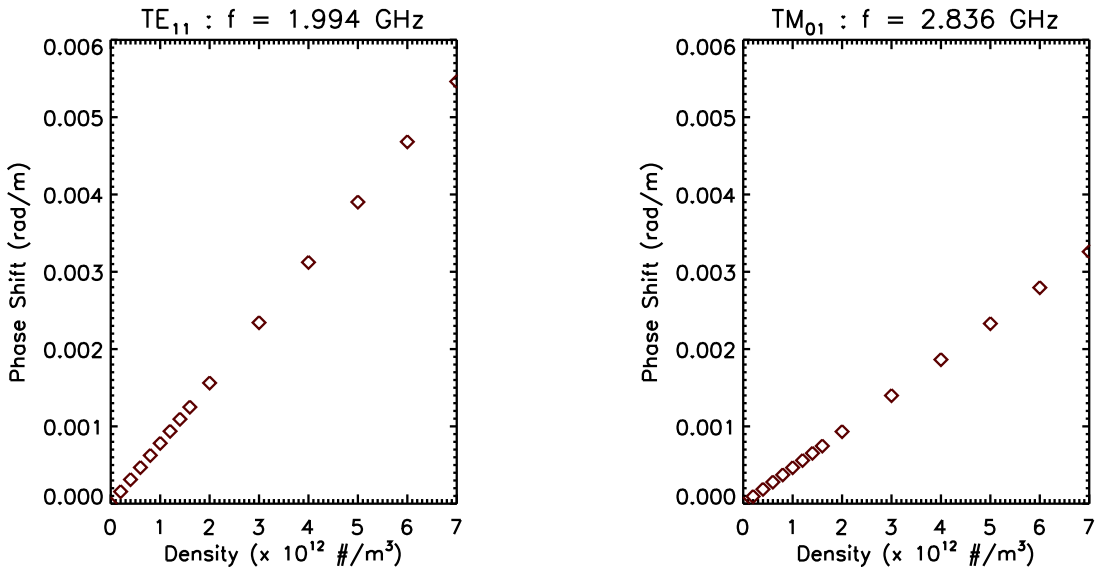

Figure 4: Phase shifts as a function of electron cloud density for TE11 and TM01 modes in a simulated circular cross section beam pipe. Phase shift per unit length is linear with cloud density, and the overall magnitude of the phase shift for TE11 modes is larger than for TM01.

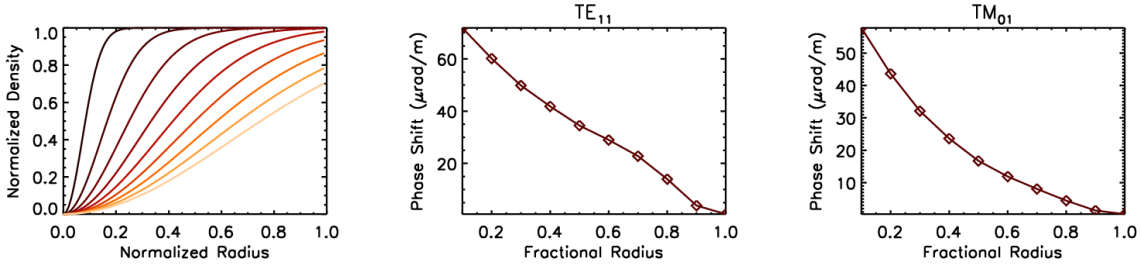

Figure 5: Phase shifts for nonuniform electron clouds for TE11 and TM01 modes. The phase shift is shown as a function of the factor f in equation (1). In both cases, the phase shift decreases as the cloud density peaks at greater radius.

In order to be sure that we are truly measuring the effect of non-uniformity in the density with higher-order modes, we further modified the simulations so that instead of rings with constant area and uniform density, the electrons were distributed in rings with a Gaussian density. The results for TE13 modes are shown in figure (7), bottom right plot. No significant differences in the phase shift pattern are seen between the Gaussian density and uniform density cases. The

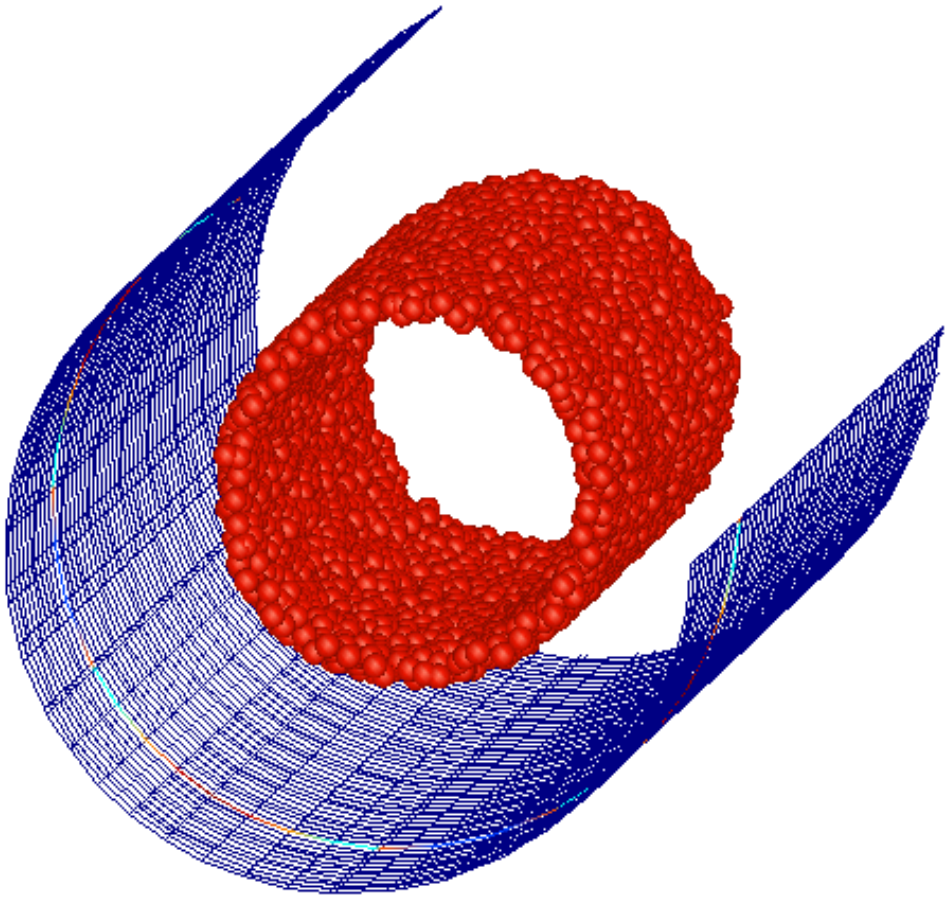

Figure 6: A typical simulation using a ring of electrons to measure the effect of non-uniformity on induced phase shifts.

overall magnitude of the phase shifts in the Gaussian case are higher because we kept the total number of electrons in the cloud constant between the uniform density case and this case. Since the peak of the Gaussian is smaller in radial extent than in the uniform density case, the peak density is also greater. Equivalence between the uniform and Gaussian density cases is a good indication that this method is not sensitive to the exact form of density non-uniformity. Based on this we believe that it is possible to use detailed simulations of higher-order modes injected into highly non uniform clouds in order to determine how to use injection of multiple modes at once to determine cloud densities in real accelerator systems.

Task 3: Study the effect of external magnetic fields on electron-cloud-induced phase shifts

We successfully completed this task in the Phase I project. In this task we simulated the transmission of both TE and TM modes though uniform, cold electron clouds while applying external magnetic fields in various directions. An applied dipole in the transverse direction has been used

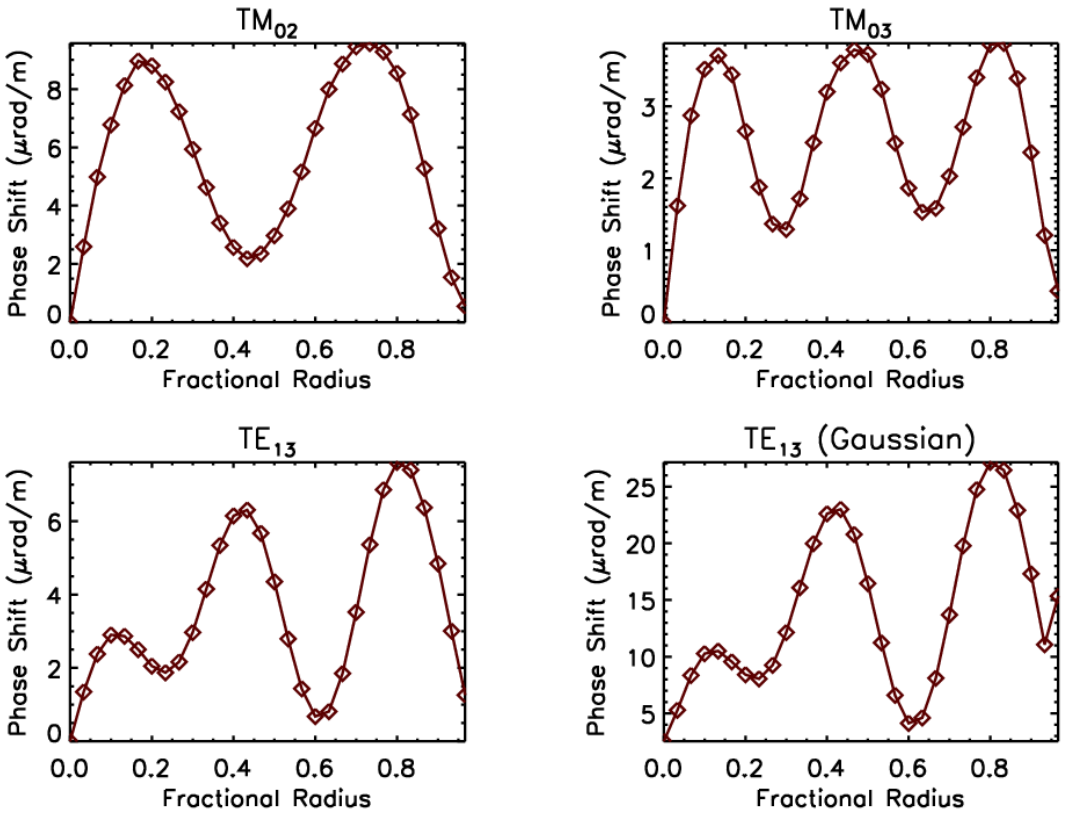

Figure 7: Higher-order modes in non-uniform electron clouds.

to measure the cyclotron resonance [5] and we undertook simulations to understand this effect. Applied solenoidal magnetic fields, in the propagation direction, are a strong candidate for mitigation of electron cloud effects if they can be shown to confine secondary electrons near the beam pipe walls instead of getting into the path of the beam. Our simulations indicated that even small solenoidal fields can reduce the number of secondary electrons significantly. However, the existence of a transverse dipole magnetic field can overwhelm this effect in real accelerator situations.

We first compared the induced phase shift for the case of an applied dipole magnetic field in the transverse direction (perpendicular to the beam propagation direction) while applying a TE11 mode. We chose the direction to also be perpendicular to the electric field of the RF wave, in order to excite the upper hybrid wave resonance. In previous simulations using square cross section beam pipes we we able to make some measurements of this resonance, referred to as the cyclotron resonance, and we were able to similarly measure the resonance in this case with circular cross sections.

Figure (8) shows the resonance in the phase shift as a function of applied field strength, for TE11 and TM01 modes. The upper two plots show the cyclotron resonance when the applied magnetic field is in the z-direction. In these simulations the TE11 mode was polarized in the y-direction, so in that case (upper left), the applied magnetic field excites the upper hybrid resonance. The lower two plots show the resonance when the applied magnetic field is in the y-

direction. We expected no resonance to be seen for the TE11 mode in this case. The existence of a very small resonance is due to small numerical errors which provide a very small z-component of electric field in the TE11 mode. In both cases for TM01 modes however, a resonance is seen. This is because for the TM01 mode, while the magnitude of the electric field is largest in the x-direction (propagation direction), there is an electric field in both of the transverse directions with about the same strength. Thus the cyclotron resonance can be seen no matter which direction the applied magnetic field is pointing.

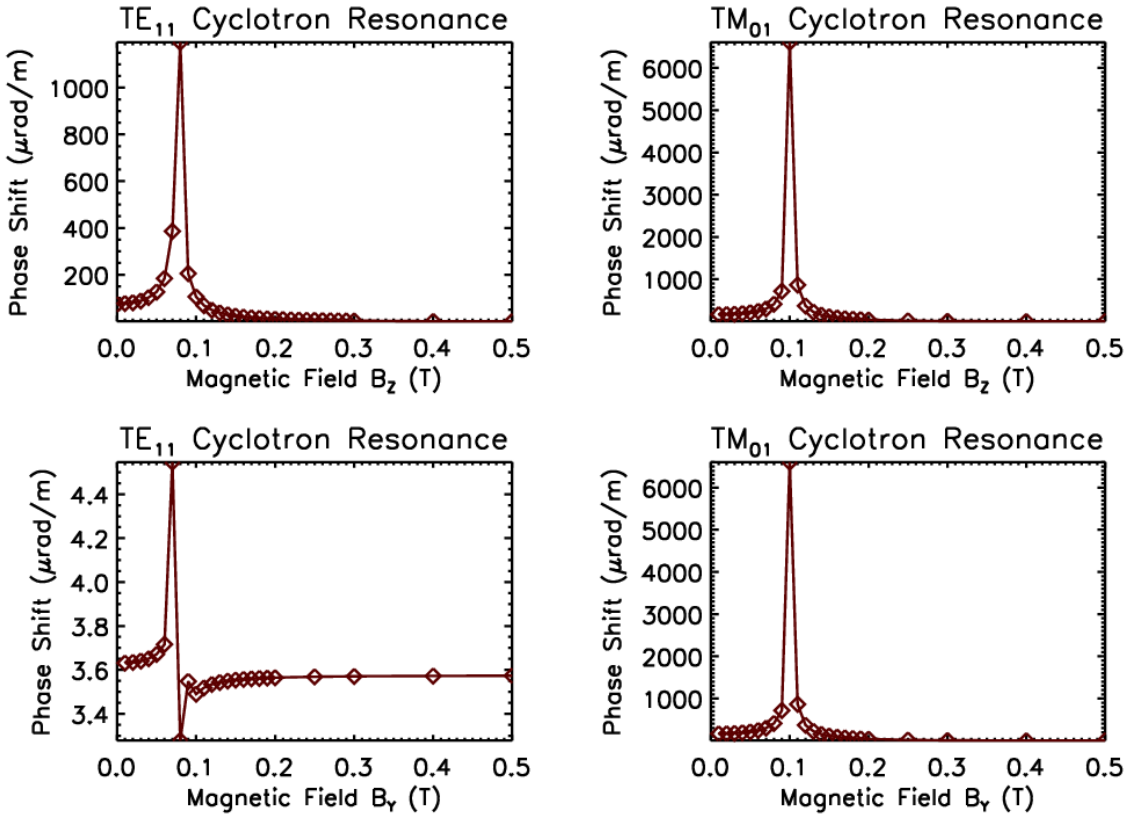

Figure 8: Cyclotron resonance in the phase shift as a function of applied field strength.

Notice from the figure that the field strength at which the resonance peaks is slightly different between TE11 and TM01 modes. This is because in these simulations we drive the RF signals at 10% above the cutoff frequency for each mode, and the cut off frequencies are different for the different modes. Here, the ratio of TM01 frequency to TE11 frequency is about

$$R = \frac{2.836GHz}{2.172GHz} \approx 1.3. \tag{2}$$

Indeed, looking at figure (8) the resonance for the TM01 mode is about 30% higher than that for the TE11 mode. It may be possible in the future to exploit this difference in the field strength that produces the cyclotron resonance in an experiment that injects both TE and TM modes with an external magnetic field. One can also imagine a situation where the resonance might be split by injecting two RF signals with slightly different frequencies and applying a

single dipole field near the peak of the cyclotron resonance. This would enable researchers to more accurately deduce the electron cloud density than by just measuring the phase shift at a single frequency, without an externally applied magnetic field.

Applied magnetic fields in the direction of propagation may be useful for reducing the negative effects of electron clouds in accelerators. The solenoidal fields are effective at confining the electrons which may be beneficial in two ways. First, for electrons that are created at the walls of the beam pipe due to secondary electron processes, the electrons can not travel to the center of the beam pipe and interfere with the beam itself. Without a confining magnetic field, the positive potential of the beam would attract secondary electrons to the center, both interfering with the beam, and giving kinetic energy to the electrons, which may then hit the opposite wall and create yet more electrons. Second, electrons that stay near the beam pipe wall have a smaller secondary electron yield than ones that travel across the beam pipe because they have a lower kinetic energy. It has been observed that a solenoidal field as small as 10 Gauss can effectively suppress the formation of electron clouds [6].

We also performed simulations of electron clouds in elliptical beam pipes with applied solenoidal fields and the influence of beam bunches. These simulations were done in conjunction with researchers at FermiLab who are interested in determining the potential problems that electron clouds may cause when the Main Injector is upgraded to higher power. We first performed simulations over a time scale of $1\mu s$ with no applied magnetic fields, and an initially uniform density electron clouds of nominal density $2.5e^{11}e^{-}/m^{3}$. In these simulations, electrons are attracted to the center of the beam pipe by the positive potential of the beam bunches, and impact the beam pipe walls, creating secondary electrons. For comparison, we repeated the simulations with a 10 Gauss solenoidal field applied to the system.

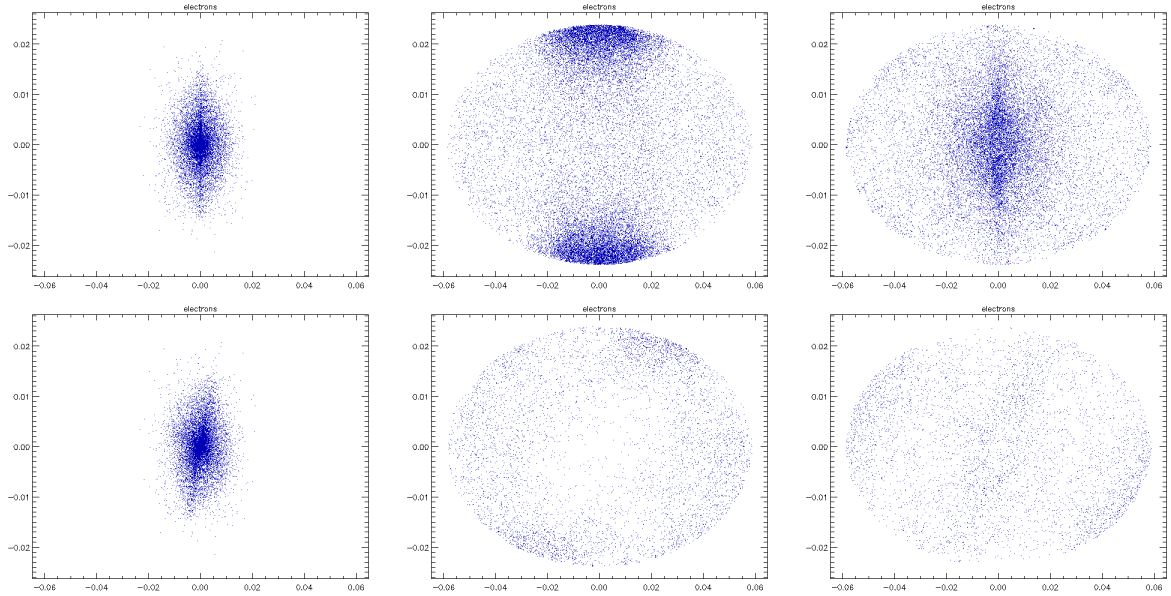

Figure 9: Transverse projections of electrons in the presence of beam currents, with no applied magnetic fields (top row) and with a 10 Gauss solenoidal field (bottom row).

A comparison of the electron positions is shown in figure (9). The top row shows the electrons

at three times in the case of no applied magnetic field. The bottom row shows the electrons at the same times with an applied 10 Gauss solenoidal field. The left figures show the electron cloud during the first beam crossing, about 17 ns after the start of the simulation. The middle figures show the clouds at about $0.5\mu s$, and the right figures are at a simulation time of about $1.0\mu s$. The results indicate that applying a solenoidal magnetic field is effective at reducing the effects of electron clouds, in this case primarily because the number of secondary electrons is greatly reduced. The total number of electrons in the simulation after $1\mu s$ is about a factor of four less than in the case with no applied magnetic field.

We also performed similar simulations with a 10 Gauss solenoidal field, and an additional external dipole magnetic field of 2340 Gauss. This is the ambient dipole field that is found in the Main Injector. In this case, almost all of the confinement effects of the solenoidal field were overwhelmed by the dipole field, and the overall electron cloud density was not reduced compared to the no magnetic field case.

Additional Accomplishments

Direct modeling support for FNAL Main Injector

Recent research efforts at FermiLab to model electron clouds in the Main Injector (MI) are very synergistic with this project. The MI has elliptical beam pipes, with a major to minor radius ratio of about 2:1. Researchers at FNAL are primarily interested in the long term evolution of electron clouds in the MI, and are in the process of fielding an RF diagnostic to measure electron clouds as well. Subsequently we have been collaborating with researchers at FNAL to develop detailed simulations of electron clouds in the MI using VORPAL. These simulations include elliptical cross section beam pipes with cut-cell geometry, thermalized electron clouds, a small transverse dipole field as is actually seen in the MI, injection of RF diagnostic waves, and accurate representations of beam currents.

Long-timescale simulations (many bunch crossings) have been run, and are continuing to be run by FNAL researchers using VORPAL, simulating clouds in a 5 m section of beam pipe. These simulations have been done in serial for smaller problems, and are also being done in parallel on the leadership-class BlueGene/P clusters at Argonne National Laboratory, and on Tech-X computational clusters. Tech-X has been providing access to VORPAL and technical support, as well as scientific collaboration in this modeling effort.

Papers and Presentations

There have been a number of papers and conference presentations on the work that was done in the Phase I project. Preliminary results using VORPAL on the simulation of phase shifts in magnetic-free and dipole regions for square cross section cavities appeared in the Proceedings of EPAC08 [6]. Results showing transmission of higher order modes in circular beam pipes was also presented at the EPAC08 conference [7]. Recent research results from the Phase I project on the measurement of cyclotron resonances and the measurement of non-uniformity using higher-order modes was presented at the PAC09 conference [8], as well as simulations of electron cloud buildup in the Main Injector [9]. We also presented our results from the Phase I project at the SciDAC 2009 conference in an invited poster. These results were published in the conference proceedings (peer reviewed) [10].

References

[1] T. Kroyer, "Application of waveguide mode diagnostics for remote sensing in accelerator beam pipes", CERN-THESIS-2005-061, Vienna Tech. U., Aug 2005.

[2] T. Kroyer, F. Caspers, E. Mahner and T. Wien, "The CERN SPS experiment on microwave transmission through the beam pipe", *Proceedings of PAC05*, 2005.

[3] J. Byrd, S. De Santis, K. Sonnad and M. Pivi, "Measurements of the propagation of EM waves through the vacuum chamber of the PEP-II low energy ring for beam diagnostics", *Proceedings of PAC07*, 2007.

[4] C. Nieter and J.R. Cary, "VORPAL: A versatile plasma simulation code", *J. Comput. Phys.*, **196**, pp. 448-473, 2004.

[5] M. Pivi et. al., "Secondary electron yield and groove chamber tests in PEP-II", *Proceedings of PAC07*, 2007.

[6] M. T. F. Pivi et. al., "Microwave transmission measurement of the electron cloud density in the positron ring of PEP-II", *Proceedings of EPAC08*, 2008.

[7] S. A. Veitzer, K. G. Sonnad, P. H. Stoltz and J. R. Cary, "Numerical modeling of microwave transmission techniques as a diagnostic for electron clouds", *Proceedings of EPAC08*, 2008.

[8] S. A. Veitzer, K. G. Sonnad, P. H. Stoltz and J. Byrd, "Modeling Microwave Transmission in Electron Clouds", *Proceedings of PAC09*, 2009.

[9] P. Lebrun, P. Stoltz and S. A. Veitzer "Microwave Transmission through the Electron Cloud at the Fermilab Main Injector: Simulation and Comparison with Experiment", *Proceedings of PAC09*, 2009.

[10] S. A. Veitzer et. al., "Computation of electron cloud diagnostics and mitigation in the Main Injector", *J. Phys.: Conf. Series*, **180**, 012007, doi:10.1088/1742-6596/180/1/012007, 2009.